Plastic Strain and Grain Size Effect on High-Pressure Phase Transformations in Nanostructured TiO$_2$ Ceramics

Hadi Razavi-Khosroshahi[1,*], Kaveh Edalati[2,3], Mokoto Arita[3],
Zenji Horita[2,3] and Masayoshi Fuji[1]

[1] Advanced Ceramics Research Center, Nagoya Institute of Technology, Gifu 507-0033, Japan

[2] WPI, International Institute for Carbon-Neutral Energy Research (WPI-I2CNER), Kyushu University, Fukuoka 819-0395, Japan

[3] Department of Materials Science and Engineering, Faculty of Engineering, Kyushu University, Fukuoka 819-0395, Japan

Anatase TiO$_2$ was severely deformed using high-pressure torsion and the effect of plastic strain and grain size on phase transformations was investigated. A high-pressure TiO$_2$-II phase (columbite) with the orthorhombic structure was formed under pressures of 1 and 6 GPa. Fraction of TiO$_2$-II increased with increasing the plastic strain and remained stable at ambient pressure. Microstructural analysis showed that TiO$_2$-II was stabilized in grains with sizes less than ~15 nm because of high energy barrier for reverse phase transformation, while larger grains had the anatase structure. Large densities of oxygen vacancies and dislocations were also formed after severe plastic deformation.

*Corresponding author: Hadi Razavi-Khosroshahi
E-mail: razavi.khosroshahihadi@nitech.ac.jp, Tel: +81-572-24-8110, Fax: +81-572-24-8109

TiO$_2$ exists in three main polymorphs under ambient condition: rutile and anatase with the tetragonal structure, and brookite with the orthorhombic structure [1-6]. Both anatase and brookite are metastable and transform to rutile at higher temperatures [1]. In addition to temperature, pressure also causes phase transformations in TiO$_2$. Anatase transforms to TiO$_2$-II (columbite) with the orthorhombic structure at 2.5-7 GPa [1-4] and to baddeleyite with the monoclinic structure at 12-15 GPa [5,6]. Recently, high-pressure phases of TiO$_2$ are receiving appreciable attention because of their narrow band gap, which makes them potential photocatalysts under visible light [7]. However, stabilizing these phases at ambient pressure is a challenging task.

Although the effect of temperature and pressure on allotropic phase transformation of TiO$_2$ is well studied [1-6], the effect of plastic strain as a factor that can cause phase transformation is not well understood. Earlier experiments using shock wave compression [8] and high-energy ball milling [9-12] suggested that the plastic strain accelerates the phase transformations in TiO$_2$.

Size effect is another factor which influence the phase transformations in TiO$_2$. Smaller particles usually exhibit more sluggish phase transformations both at high temperatures [13,14] and high pressures [15,16]. Reidy *et al.* [14] reported a minimum critical particle size of 45 nm for anatase to rutile transition under ambient pressure. Theoretical study conducted by Hearne *et al.* [17] concluded that coarse-grained anatase underwent a

transformation from anatase to TiO_2-II at 5 GPa, and from TiO_2-II to baddeleyite at 15 GPa. Whilst, anatase with an average grain size of ~12 nm did not transform to TiO_2-II, but transformed to baddeleyite directly at 18 GPa. Other studies showed that anatase with sizes at nanometer level hardly transformed to TiO_2-II or baddeleyite [18-20]. Most of the cited experimental studies [15-20] are on the relation between particle size and phase transformation. However, the effect of grain size on the stability of high-pressure TiO_2 phases at ambient pressure is not well understood.

The high-pressure torsion (HPT) method [21], in which the material is compressed between two anvils under controllable pressures and plastic strain is induced by rotating the two anvils against each other, is an ideal technique to investigate the simultaneous effect of pressure, plastic strain and grain size on phase transformations. Although the HPT method is mainly used to achieve nanograins [22-24] and metastable or stable phases [25-27] in metallic materials, there have been several attempts to use the method for processing ceramics [21,28-30].

In this study, anatase TiO_2 is processed by HPT under hydrostatic pressures of 1 and 6 GPa and the effect of plastic strain and grain size on the stability of TiO_2-II phase at ambient pressure is investigated. Pressures of 1 and 6 GPa are selected below and above the reported critical pressure for anatase to TiO_2-II transition, 2.5-7 GPa [1-4].

Starting material was anatase TiO_2 powders with a purity level of 99.8% and ~150

3

nm particle size. Almost 0.2 g of powders were placed between two Bridgman anvils [21] under $P = 1$ and 6 GPa and shear strain γ ($\gamma = 2\pi r N/h$; r: distance from disc center, N: number of turns, h: sample thickness [22]) was introduced by rotating the two anvils with respect to each other for either 0 (mere compression), 1/16, 1/4, 1 and 4 turns at room temperature. After HPT processing, the material had a disc shape with 10mm diameter and 0.8mm thickness. The HPT-processed discs were polished and examined in terms of (i) X-ray diffraction (XRD) analyses using the CuKα radiation, (ii) Raman spectroscopy at 3 mm from the center of discs using a micro-Raman system with a 532 nm solid state laser, (iii) photoluminescence (PL) spectroscopy using a spectrofluorometer equipped with a Xenon lamp with an excitation wavelength of 350 nm, and (iv) high-resolution transmission electron microscopy (TEM). Thin foils for TEM were prepared by crushing the edge part of samples and pouring them on a carbon-type grid.

XRD results for samples processed by HPT under 1 and 6 GPa for 4 turns are shown in Fig. 1(a). Anatase peaks are clearly visible in powder and in the HPT-processed samples, while a distinct peak broadening occurs after HPT processing. This peak broadening is an indication of lattice strain, which results from the formation of lattice defects. In addition to anatase, TiO_2-II can also be detected for samples processed by HPT. The TiO_2-II phase remained stable for at least 200 days under ambient condition. It is noteworthy that TiO_2-II phase was formed even under 1 GPa, which is below the reported critical pressure for TiO_2-II

formation at room temperature (2.5-7 GPa [1-4]). Such a decrease in transition pressure should be due to the effect of plastic strain.

The effect of plastic strain on phase transformation is shown more clearly in XRD results of Figs. 1(b) and (c). The intensity of TiO_2-II peaks and the fraction of TiO_2-II (obtained from Rietveld analysis) increase as the number of HPT turns and plastic strain increase. The trend of phase fraction against strain in Fig. 1(c) is similar to those observed in HPT-processed metallic materials [23-24] and ceramics [28-30]. The effect of plastic strain on phase transformation can be also confirmed by Raman spectroscopy, as shown in Fig. 2(a). Vibration modes for anatase can be seen in the samples before and after HPT processing, while TiO_2-II peaks appear only after HPT processing and their intensity increases with increasing the strain. Details of Raman spectroscopy for anatase and TiO_2-II were reported elsewhere [2,31]. The current results together with the earlier reports achieved by shock wave compression [8] and high-energy ball milling [9-12] confirm that the plastic strain has a significant effect to overcome the energy barrier for anatase to TiO_2-II transition.

Photos of HPT-processed discs are embedded in Fig. 1(c). The color of sample after pure compression is white (the same color as that of the powder), but the color changes to dark green after HPT processing, indicating that oxygen vacancies are formed [32]. PL spectroscopy, as shown in Figure 2(b), is a powerful technique to investigate the condition of vacancies in semiconductors by examination of the charge carrier trapping, immigration and

recombination [33]. The PL plateau centered at $\lambda = 430$ and 470 nm in Fig. 2(b) are due to the band-band transition photoluminescence and the shallow traps on oxygen vacancies, respectively [34]. It is clear that PL intensity increases as the number of HPT turns increases, indicating that the oxygen vacancy concentration increases. Earlier reports also showed that supersaturated vacancies are formed in metallic materials by severe plastic deformation [35].

A representative bright-filed TEM image of powder and corresponding selected-area electron diffraction (SAED) pattern are shown in Figs. 3(a) and (b), respectively. The average grain size is 150±30 nm and all diffraction spots in the SAED pattern correspond to the anatase phase. Whilst, the material processed by HPT for 4 turns has a bimodal microstructure composed of large grains with sizes larger than 40 nm and small grains with sizes in the range of 5-15 nm. Careful examination of large grains (as shown in Fig. 3(c)) indicates that they have an anatase structure and several edge dislocations are visible within these grains, but the small nanograins (as shown in Fig. 3(e)) have a TiO_2-II structure. Edge dislocations are marked by T in Fig. 3(c) and shown more clearly in the lattice image of Fig. 3(d) obtained by inverse fast Furrier transform (FFT). The presence of six dislocations in Fig. 3(c) within a small area of 2600 nm^2 corresponds to a high dislocation density of 2.3x10^{15} m^{-2}. Such a high dislocation density is anomalous for most ceramics and is comparable to those reported in severely deformed metallic materials [22,23]. Examination results of 80 grains using high-resolutions TEM are summarized in Fig. 4. As shown, nanograins with sizes less than 15

nm always have a TiO$_2$-II structure, while larger grains have an anatase structure. The formation of nanograins in this study is well consistent with the earlier reports on HPT processing of other ceramics such as ZrO$_2$ [28] and BaTiO$_3$ [30].

Two questions naturally arise from the current study: why TiO$_2$-II remained stable at ambient pressure and why it formed under pressures as low as 1 GPa? Microstructural analyses in Figs. 3 and 4 clearly indicate that the stability of TiO$_2$-II phase is due to the grain size effect, which is in good agreement with the earlier reports in HPT-processed Co [36], Ti [27] and BaTiO$_3$ [30]. According to literature, pressure- and temperature-induced phase transformations in TiO$_2$ are suppressed when the particle size is well at the nanometer level [15-20]. Hearne *et al.* [17] calculated the critical grain size for the nucleation of orthorhombic TiO$_2$-II phase at the interface of anatase grains and concluded that TiO$_2$-II nucleated only for anatase grains that have sizes larger than 12 nm. They suggested that the energy barrier for nucleation of TiO$_2$-II at the boundaries of small anatase grains was too high, so that the anatase/TiO$_2$-II interfaces became energetically unfavorable. In agreement with Ref. [17], TiO$_2$-II remained stable in grains smaller than 15 nm because of the energy barrier for nucleation of anatase which makes the anatase/TiO$_2$-II interfaces energetically unfavorable.

The formation of TiO$_2$-II under 1 GPa, which is appreciably below the critical pressure for the formation of TiO$_2$-II under pure compression (2.5-7 GPa [1-4]), clearly proves that strain plays a significant role on overcoming the energy barrier for nucleation of

TiO_2-II. It is important to note that in pure compression without strain, new phases nucleate at lattice defects such as dislocations that already exist in the material [37]. Since the fraction of these defects is usually limited, high pressures are needed to overcome the energy barrier for nucleation. In contrast, in HPT a huge population of new defects continuously generate during plastic deformation [38]. Therefore, nucleation sites are abundant and thus the pressure required for phase transformation becomes lower. The pile-up of lattice defects such as dislocations at grain boundaries also provides an effective pressure tensor concentrator, which can reduce the threshold for phase transformation. In addition, the presence of point defects such as vacancies enhances the atomic mobility for phase transformation.

In summary, anatase TiO_2 transformed to orthorhombic TiO_2-II after HPT processing under pressures of 1 and 6 GPa, and the fraction of TiO_2-II increased with increasing the strain. The TiO_2-II phase with grain sizes smaller than ~15 nm remained stable for at least 200 days at ambient pressure. The current study introduces a new mechanism for stabilization of TiO_2-II phase, whose photoactivity is recently receiving appreciable attention [7].

References

[1]   F. Dachille, P.Y. Simons, R. Roy, Am. Mineral. 53 (1968) 1929-1939.

[2]   T. Ohsaka, S. Yamaoka and O. Shimomura, Solid State Commun. 30 (1979) 345-347.

[3]   K. Lagarec, S. Desgreniers, Solid State Commun. 94 (1995) 519-524.

[4]   T. Arlt, M. Bermejo, M.A. Blanco, L. Gerward, J. Jiang, J.S. Olsen, J.M. Recio, Phys. Rev. B 61 (2000) 14414-14419.

[5]   P.Y. Simons, F. Dachille, Acta Crystallogr. 23 (1967) 334-336.

[6]   J.C. Jamieson, B. Olinger, Science 161 (1968) 893-895.

[7]   M.Y. Kuo, C.L. Chen, C.Y. Hua, H.C. Yang, P. Shen, J. Phys. Chem. B, 109 (2005) 8693-8700.

[8]   R.G. McQueen, J.C. Jamieson, S.P. Marsh, Science 155 (1967) 1401-1404.

[9]   J. Chaudhuri, M. Ram, B. Sarkar, J. Mater. Sci. 29 (1994) 3484-3488.

[10]   S. Begin-Colin, T. Girot, A. Mocellin, G. Le Caër, Nanostruct. Mater. 12 (1999) 195-198.

[11]   H. Dutta, P. Sahu, S. Pradhan, M. De, Mater. Chem. Phys. 77 (2003) 153-164.

[12]   E. Napolitano, G. Mulas, S. Enzo, F. Delogu, Acta Mater. 58 (2010) 3798-3804.

[13]   H. Zhang, J.F. Banfield, J. Phys. Chem. B 104 (2000) 3481-3487.

[14]   D.J. Reidy, J.D. Holmes, M.A. Morris, J. Eur. Ceram. Soc. 26 (2006) 1527-1534.

[15]   V. Pischedda, G.R. Hearne, A.M. Dawe, J.E. Lowther, Phys. Rev. Lett. 96 (2006) 035509.

[16]   V. Swamy, A. Kuznetsov, L.S. Dubrovinsky, P.F. McMillan, V.B. Prakapenka, G.Y. Shen, B.C. Muddle, Phys. Rev. Lett. 96 (2006) 135702.

[17]   G.R. Hearne, J. Zhao, A.M. Dawe, V. Pischedda, M. Maaza, M.K. Nieuwoudt, P. Kibasomba, O. Nemraoui, J.D. Comins, M.J. Witcomb, Phys. Rev. B 70 (2004) 134102.

[18]   V. Swamy, A. Kuznetsov, L.S. Dubrovinsky, R.A. Caruso, D.G. Shchukin, B.C. Muddle, Phys. Rev. B 71 (2005) 184302.

[19] Z. Wang, S.K. Saxena, Solid State Commun. 118 (2001) 75-78.

[20] Z. Wang, S.K. Saxena, V. Pischedda, H.P. Liermann, C.S. Zha, J. Phys.: Condens. Mater. 13 (2001) 8317-8323.

[21] P.W. Bridgman, Phys. Rev. 48 (1935) 825-847.

[22] R.Z. Valiev, Y. Estrin, Z. Horita, T.G. Langdon, M.J. Zehetbauer, Y.T. Zhu, JOM 58 (4) (2006) 33-38.

[23] A.P. Zhilyaev, T.G. Langdon, Prog. Mater. Sci. 53 (2008) 893-979.

[24] R. Pippan, S. Scheriau, A. Taylor, M. Hafok, A. Hohenwarter, A. Bachmaier, Annu. Rev. Mater. Res. 40 (2010) 319-43.

[25] A.P. Zhilyaev, I. Sabirov, G. Gonzales-Doncel, J. Molina-Aldarequia, B. Srinivasarao, M.T. Perez-Prado, Mater. Sci. Eng. A 528 (2011) 3496-3505.

[26] N.Q. Chinh, R.Z. Valiev, X. Sauvage, G. Varga, K. Havancsak, M. Kawasaki, B.B. Straumal, T.G. Langdon, Adv. Eng. Mater. 16 (2014) 1000-1009.

[27] K. Edalati, T. Daio, M. Arita, S. Lee, Z. Horita, A. Togo, I. Tanaka, Acta Mater. 68 (2014) 207-213.

[28] K. Edalati, S. Toh, Y. Ikoma, Z. Horita, Scripta Mater. 65 (2011) 974-977.

[29] V.I. Levitas, Y. Ma, E. Selvi, J. Wu, J.A. Patten, Phys. Rev. B 85 (2012) 054114.

[30] K. Edalati, M. Arimura, Y. Ikoma, T. Daio, M. Miyata, D.J. Smith, Z. Horita, Mater. Res. Lett. 3 (2015) 216-221.

[31] T. Ohsaka, F. Izumi, Y. Fujiki, J. Raman Spectrosc. 7 (1978) 321-324.

[32] T. Sekiya, T. Yagisawa, N. Kamiya, D. Das Mulmi, S. Kurita, Y. Murakami, T. Kodaira, J. Phys. Soc. Jpn. 73 (2004) 703-710.

[33] C.C. Mercado, F.J. Knorr, J.L. McHale, S.M. Usmani, A.S. Ichimura, L.V.J. Saraf, Phys. Chem. C 116 (2012) 10796-10804.

[34] J. Yan, G. Wu, N. Guan, L. Li, Z. Li, X. Cao, Phys. Chem. Chem. Phys. 15 (2013) 10978-10988.

[35] B. Oberdorfer, B. Lorenzoni, K. Unger, W. Sprengel, M. Zehetbauer, R. Pippan, R. Wurschum, Scripta Mater. 63 (2010) 452-455.

[36] K. Edalati, S. Toh, M. Arita, M. Watanabe, Z. Horita, Appl. Phys. Lett. 102 (2013) 181902.

[37] V.I. Levitas, Phys. Rev. B 70 (2004) 184118.

[38] V.I. Levitas, M. Javanbakht, Nanoscale 6 (2014) 162-166.

Figure captions

Figure 1. (a) XRD patterns for powders and samples processed by HPT under 1 and 6 GPa for 4 turns, (b) XRD patterns for powders and samples processed by HPT under 6 GPa for various turns, and (c) fractions of anatase and TiO_2-II as a function of shear strain.

Figure 2. (a) Raman and (b) PL spectra for powders and samples processed by HPT under 6 GPa for various turns.

Figure 3. (a) Bright-field TEM image and (b) corresponding SAED pattern for anatase powders; (c-e) high-resolution TEM images of sample processed by HPT under 6 GPa for 4 turns. (c) corresponds to anatase grain (dislocations inside the grain are marked with T); (d) corresponds to lattice image of edge dislocation in anatase grain obtained by inverse FFT and (e) corresponds to TiO_2-II nanograins (difractograms for grains A, B and C are shown in (e)).

Figure 4. A histogram of grain size distribution for anatase and TiO_2-II phases in sample processed by HPT under 6 GPa for 4 turns.
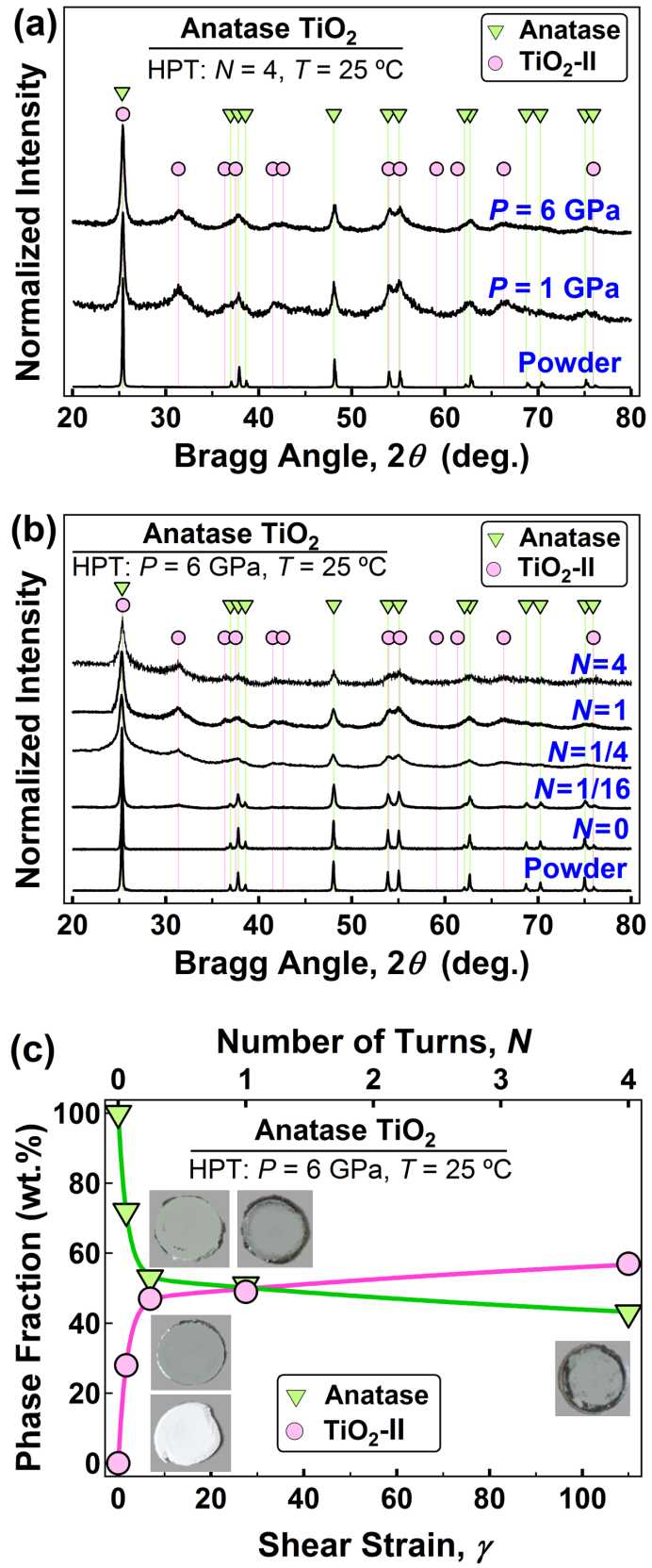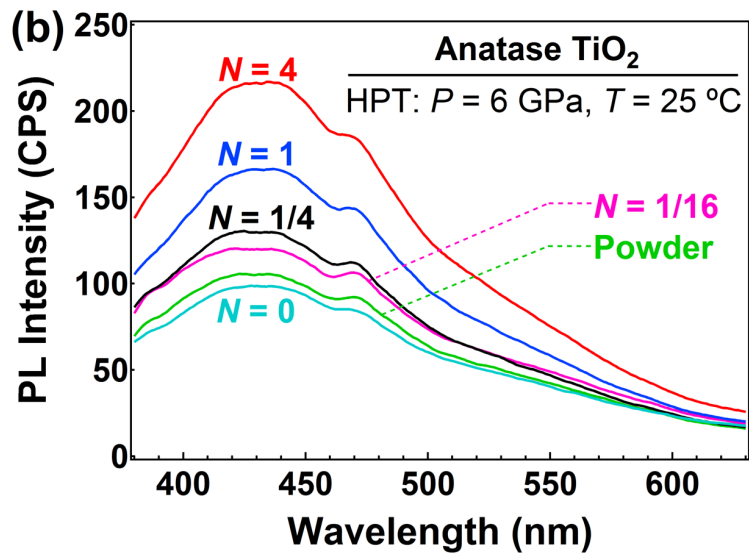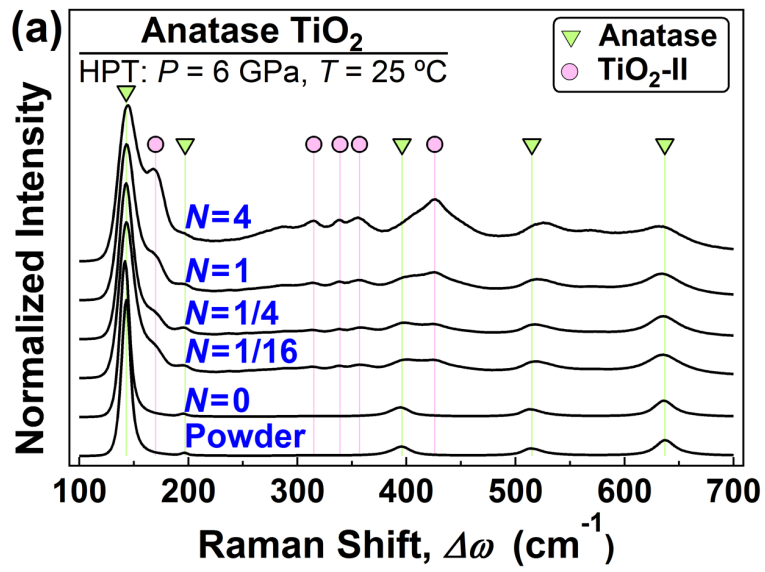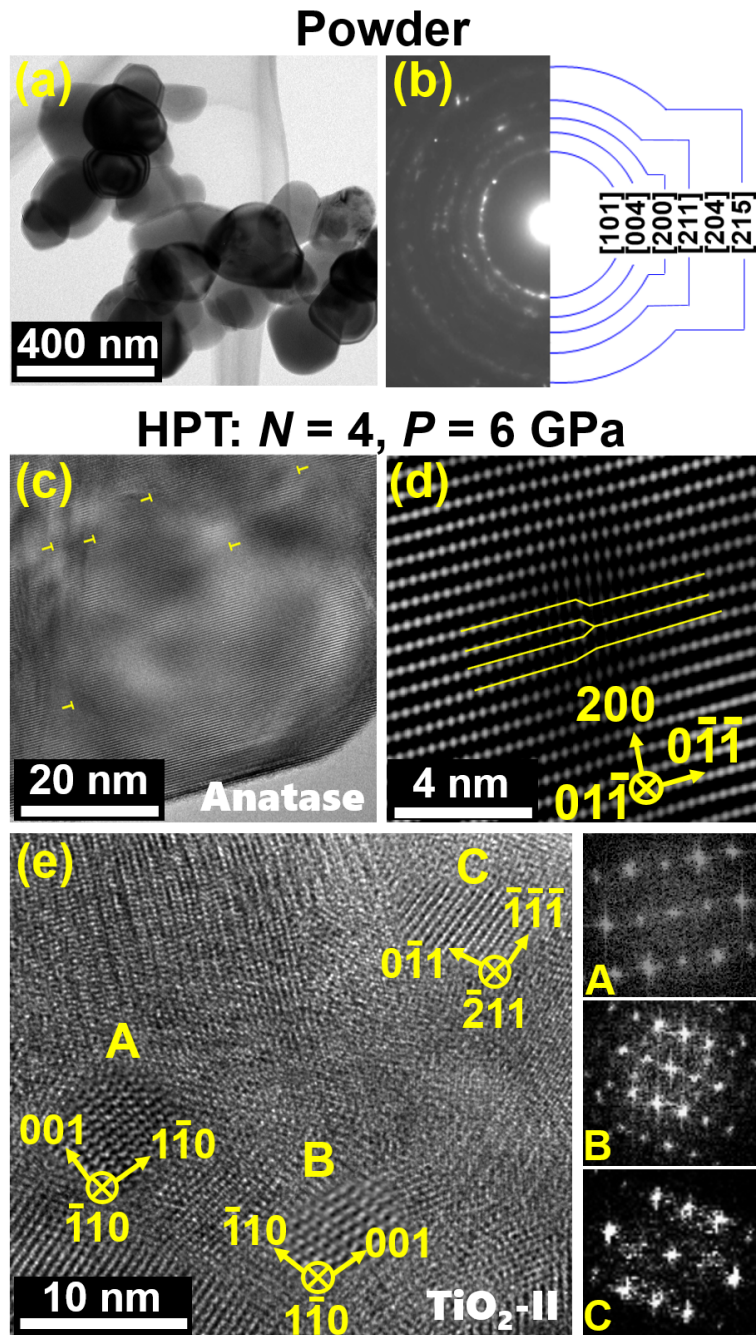
Figure 1

Figure 2

Powder

HPT: N = 4, P = 6 GPa

Figure 3

Figure 4